HHS Public Access

Author manuscript

Mol Microbiol. Author manuscript; available in PMC 2018 October 01.

Published in final edited form as:

Mol Microbiol. 2017 October ; 106(2): 319–333. doi:10.1111/mmi.13766.

The inositol pyrophosphate synthesis pathway in *Trypanosoma brucei* is linked to polyphosphate synthesis in acidocalcisomes

Ciro D. Cordeiro[1], **Adolfo Saiardi**[2], and **Roberto Docampo**[1,#]

[1]Center for Tropical and Emerging Global Diseases and Department of Cellular Biology, University of Georgia, Athens, Georgia, 30602, USA

[2]Medical Research Council Laboratory for Molecular Cell Biology, University College London, WC1E 6BT, Gower Street, London, United Kingdom

Summary

Inositol pyrophosphates are novel signaling molecules possessing high-energy pyrophosphate bonds and involved in a number of biological functions. Here, we report the correct identification and characterization of the kinases involved in the inositol pyrophosphate biosynthetic pathway in *Trypanosoma brucei*: inositol polyphosphate multikinase (TbIPMK), inositol pentakisphosphate 2-kinase (TbIP5K) and inositol hexakisphosphate kinase (TbIP6K). TbIP5K and TbIP6K were not identifiable by sequence alone and their activities were validated by enzymatic assays with the recombinant proteins or by their complementation of yeast mutants. We also analyzed *T. brucei* extracts for the presence of inositol phosphates using polyacrylamide gel electrophoresis and high performance liquid chromatography. Interestingly, we could detect inositol phosphate (IP), inositol 4,5-bisphosphate (IP_2), inositol 1,4,5-trisphosphate (IP_3) and inositol hexakisphosphate (IP_6) in *T. brucei* different stages. Bloodstream forms unable to produce inositol pyrophosphates, due to downregulation of *TbIPMK* expression by conditional knockout, have reduced levels of polyphosphate and altered acidocalcisomes. Our study links the inositol pyrophosphate pathway to the synthesis of polyphosphate in acidocalcisomes, and may lead to better understanding of these organisms and provide new targets for drug discovery.

Graphical Abstract

We report the correct identification and characterization of the kinases involved in the inositol pyrophosphate biosynthetic pathway in *Trypanosoma brucei* and identified the substrates and products of these reactions. We provide functional evidence of their activity by complementation of yeast mutants, and we establish the relevance of this pathway for acidocalcisome polyphosphate synthesis in trypanosomes.

[#]Corresponding author: rdocampo@uga.edu, Tel: +1-706-542-8104; FAX: +1-706-542-9493.

Competing interests

The authors declare no competing or financial interests

Author contributions

C.C., A.S. and R.D. designed the experiments and analyzed the data. C.C. and A.S. conducted the experiments. R.D. wrote the majority of the manuscript, with specific sections contributed by C.C., and A.S. R.D. and A.S. supervised the work and contributed to the analysis of experiments.

Supporting information

Supplementary information available online at:

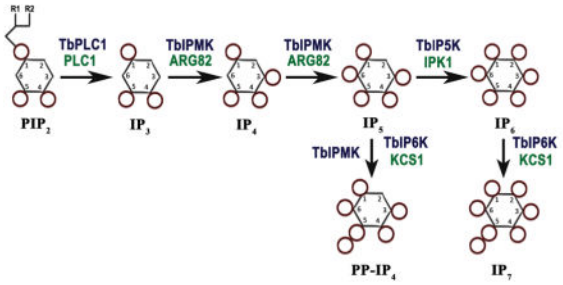

Keywords

Acidocalcisome; polyphosphate; inositol pyrophosphate; calcium; Trypanosoma brucei

Introduction

Myo-inositol is an essential precursor for the synthesis of soluble inositol phosphates (IPs) and lipid-bound inositols called phosphoinositides (PIPs) (Irvine *et al.*, 2001). After inositol incorporation into the lipid phosphatidylinositol (PI), the inositol ring is phosphorylated to PIPs such as phosphatidylinositol 4,5-bisphosphate (PIP_2) through the action of a phosphatidylinositol phosphate (PIP) kinase. PIP_2 is cleaved by a phosphoinositide phospholipase C (PI-PLC) (Cocco *et al.*, 2015) to inositol 1,4,5-trisphosphate (IP_3) (Fig. 1) and 1,2-diacylglycerol (DAG), which are important second messengers. While DAG stimulates a protein kinase C (Nishizuka, 1986), IP_3 stimulates an IP_3 receptor to release Ca^{2+} from intracellular stores (Berridge, 2009) and can be further metabolized to other soluble IPs by several kinases and phosphatases.

The inositol phosphate multikinase (IPMK) has dual 3-kinase/6-kinase activity and catalyzes the conversion of IP_3 into inositol tetrakisphosphate (IP_4) and inositol pentakisphosphate (IP_5). IP_5 is converted into inositol hexakisphosphate (IP_6), the fully phosphorylated *myo*-inositol also known as phytic acid, by the 2-kinase activity of inositol pentakisphosphate kinase (IP5K, or IPPK). Further phosphorylation of IP_6 by the inositol hexakisphosphate kinase (IP_6 kinase or IP6K) results in the production of diphosphoinositol polyphosphates (PP-IPs), also known as inositol pyrophosphates. These are IPs characterized by containing one or more high-energy pyrophosphate moiety. PP-IPs were discovered in the early 1990's, in *Dictyostelium discoideum* (Europe-Finner *et al.*, 1991, Mayr GW, 1992, Stephens *et al.*, 1993), *Entamoeba histolytica* (Martin *et al.*, 1993), and in mammalian cells (Menniti *et al.*, 1993). The best-characterized member of this class is 5-diphosphoinositol pentakisphosphate (5-PP-P_5 or IP_7), which has five of the *myo*-inositol hydroxyls monophosphorylated, while the sixth, at the 5-position, contains a pyrophosphate group (Albert *et al.*, 1997). The IP6K can also metabolize IP_5 to disphosphoinositol tetrakisphosphate (PP-IP_4) (Saiardi *et al.*, 2000, Losito *et al.*, 2009). Another isomer of IP_7, containing a pyrophosphate at the 1-position, can also be formed by a more recently identified enzyme termed diphosphoinositol pentakisphosphate kinase (PP-IP5K), though this enzyme appears to be predominantly associated physiologically with the formation of diphosphoinositol hexakisphosphate (PP_2-IP_4 or IP_8) (Choi *et al.*, 2007).

Among the many roles attributed to PP-IPs are the regulation of telomere length (Saiardi *et al.*, 2005, York *et al.*, 2005), DNA repair by homologous recombination (Luo *et al.*, 2002, Jadav *et al.*, 2013), response to hyperosmotic stress (Pesesse *et al.*, 2004, Choi *et al.*, 2007), vesicle trafficking (Saiardi *et al.*, 2000, Saiardi *et al.*, 2002), apoptosis (Morrison *et al.*, 2001, Nagata *et al.*, 2005), autophagy (Nagata *et al.*, 2010), binding of pleckstrin homology domains to phospholipids and proteins (Luo *et al.*, 2003, Gokhale *et al.*, 2013), transcription of glycolytic enzymes (Szijgyarto *et al.*, 2011), hemostasis (Ghosh *et al.*, 2013), phagocytic and bactericidal activities of neutrophils (Prasad *et al.*, 2011), epigenetic modifications to chromatin (Burton *et al.*, 2013) and exocytic insulin secretion (Illies *et al.*, 2007). PP-IPs may signal through allosteric interaction with proteins (i.e. binding to pleckstrin homology (PH) or other domains of proteins) or by phosphotransfer reactions (Saiardi, 2012, Shears, 2015, Wild *et al.*, 2016). The phosphotransfer reaction is non-enzymatic and requires a phospho-serine residue within an acidic region and consists in adding a second phosphate to the phosphor-serine resulting in pyrophosphorylation (Saiardi, 2012).

Trypanosoma brucei, which belongs to the group of parasites that causes African trypanosomiasis (sleeping sickness), possesses a PI-PLC that is stimulated by very low Ca^{2+} concentrations (King-Keller *et al.*, 2015) and an IP_3 receptor that localizes to the acidocalcisomes instead of the endoplasmic reticulum (Huang *et al.*, 2013). We now found that they also possess orthologs to IPMK, IP5K and IP6K, but do not have recognizable orthologs to PP-IP5K, inositol 1,4,5-trisphosphate 3-kinases (ITPKs) and inositol tetrakisphosphate 3-kinase 1 (ITPK1) (Table S1). The ortholog to IPMK (TbIPMK) was recently reported as essential for the bloodstream forms of the parasites (Cestari *et al.*, 2015), suggesting that the soluble inositol phosphate pathway is essential for the parasite. The orthologs to IP5K and IP6K were not recognizable by sequence only and were wrongly annotated as a putative hypothetical protein and as inositol polyphosphate-like protein, respectively. In the present study, we thoroughly characterized the soluble inositol phosphate pathway of *T. brucei*. We cloned, expressed and biochemically characterized the recombinant enzymes from *T. brucei*, complemented yeast mutants to demonstrate their function, analyzed their products, studied the inositol phosphate metabolism of *T. brucei* cells, and revealed the link of this pathway to the synthesis of polyphosphate in acidocalcisomes.

Results

Sequence analysis of T. brucei inositol phosphate kinases

Gene homology searches followed by validation of their activity (see below) have allowed to identify in the *T. brucei* genome (http://www.tritrypdb.org/tritrypdb/) the presumably gene orthologs to the inositol phosphate kinases encoding inositol polyphosphate multikinase (IPMK in mammals, and Arg82p or Ipk2p in yeast) (Tb427tmp.211.3460); the IP_5 kinase (IPPK or IP5K in mammals, and Ipk1p in yeast) (Tb427.04.1050); and the IP_6 kinase (IP6K in mammals, and Kcs1p in yeast) (Tb427.07.4400), (Fig. 1), and named *TbIPMK, TbIP5K,* and *TbIP6K*, respectively (Table S1). No orthologs to diphosphoinositol pentakisphosphate kinase (PP-IP5K in mammals, or Vip1 in yeasts) were found, although orthologs to this gene are present in Apicomplexan (Laha *et al.*, 2015) and *Giardia* (EuPathDB). The orthologs to

TbIPMK, TbIP5K, and TbIP6K identified in *T. cruzi* (TcCLB.510741.110, TcCLB.506405.90, TcCLB.504213.90) and *Leishmania major* (LmjF.35.3140, LmjF.34.3700, LmjF.14.0340) shared 45%, 36%, 35%, and 29%, 28%, 24% amino acid identity, respectively. Those of *T. brucei* share 15%, 16%, and 15% identity with the human enzymes, respectively. Structural analyses (ELM and TMHMM servers) predicted no transmembrane domains. A signal peptide was predicted for TbIP5K, but not for TbIPMK or TbIP6K. Mature proteins of 342, 461, and 756 amino acids with predicted molecular weights of 38.8, 51, and 82.6 kDa, for TbIPMK, TbIP5K, and TbIP6K, respectively, were also predicted. Amino acids 138–147 of TbIPMK, and 588–596 of TbIP6K contained the conserved sequence PCVLDL(I)KL(M)G demonstrated previously as the putative inositol phosphate binding site that catalyzes the transfer of phosphate from ATP to inositol phosphates (Bertsch *et al.*, 2000). TbIP5K possesses the sequence PVLDIELL (amino acids 269–276) instead. Both TbIPMK and TbIP6K have a SASLL or TSSLL domain present in most members of this family of enzymes and required for enzymatic activity (Saiardi *et al.*, 2001b, Nalaskowski *et al.*, 2002).

We utilized homologous recombination to add a hemagglutinin (HA) or c-Myc tag to the endogenous loci (Oberholzer *et al.*, 2006) of TbIPMK, TbIP5K and TbIP6K. All three inositol phosphate kinases are expressed in procyclic forms (PCF) of *T. brucei* (Fig. 2A). Although the predicted MW of TbIP6K is 82.6 kDa the enzyme has multiple phosphorylations (Urbaniak *et al.*, 2013) and these post-translational modifications (in addition to the HA tag) could result in a higher apparent MW. Interestingly, TbIP5K revealed no expression when using the HA-tag, but a protein with the expected size was detected when using a c-Myc tag (Fig. 2A). In addition, we tagged the three IP kinases in *T. brucei* bloodstream forms (BSF) but no clear bands were detected by western blot analyses although the tagged genes were expressed at the mRNA level (data not shown), suggesting that protein expression is lower in BSF than in PCF.

Characterization of the inositol phosphate multikinase (TbIPMK)

To characterize the enzymatic activity of TbIPMK we expressed it as fusion protein with an *N*-terminal polyhistidine tag, purified and tested its activity *in vitro*. We found that it catalyzes the formation of IP_5 from IP_3 or IP_4, as detected by polyacrylamide gel electrophoresis (Fig. 2B). Inositol-1,4,5-trisphosphate ($I(1,4,5)P_3$) but not inositol-1,3,4-trisphosphate ($I(1,3,4)P_3$) could be used as substrate while both inositol-1,3,4,5-tetraphosphate ($I(1,3,4,5)P_4$) and inositol-1,4,5,6-tetraphosphate ($I(1,4,5,6)P_4$) could be used for the generation of inositol-1,3,4,5,6-pentakisphosphate ($I(1,3,4,5,6)P_5$) (Fig. 2B), indicating that TbIPMK has a dual 3-kinase/6-kinase activity. An additional product, which runs closely but not identically to IP_6, was also detected when IP_3, IP_4, or IP_5 was used as substrate (Figs. 2B and 2C). The ability of IPMK to form PP-IP_4, an inositol pyrophosphate containing 6 phosphates and thus migrating closely to IP_6, has been demonstrated for the mammalian and yeast ortholog (Saiardi *et al.*, 2001a, Zhang *et al.*, 2001), and we therefore suspected that TbIPMK could have the same activity. A treatment with perchloric acid (PA), which degrades high-energy phosphoanhydride bonds (pyrophosphates) and is inactive against the phosphoester bond of IP_6 (Fig. 2C) (Pisani *et al.*, 2014), demonstrated that the highly phosphorylated product of TbIPMK is a pyrophosphate containing species, therefore

PP-IP_4. The pH optimum of rTbIPMK was determined. TbIPMK has the maximum activity for IP_3 at the pH range of 6.5–7.0 (Fig. 2D). We also tested the ability of TbIPMK to phosphorylate different isomers of IP_5. Recombinant TbIPMK was able to phosphorylate I(1,2,4,5,6)P_5 and I(1,2,3,4,5)P_5 to IP_6 after short incubation times, but it was not able to use I(2,3,4,5,6)P_5, I(1,3,4,5,6)P_5, (I(1,2,3,5,6)P_5, or (I(1,2,3,4,6)P_5 as substrate (Fig. 2E). Although I(1,2,4,5,6)P_5 and I(1,2,3,4,5)P_5 would not be physiological substrates, the results again confirms a 3/6-kinase activity. Interestingly, TbIPMK could also phosphorylate I(1,4)P_2 to IP_4 (Fig. 2B). The mammalian IPMK has been reported to have PI3-kinase activity that produces PIP_3 from PIP_2 (Resnick *et al.*, 2005). However, our in vitro activity tests using PIP_2 as substrate revealed no such activity (data not shown) in agreement with the results of a previous report (Cestari *et al.*, 2016).

The ability of TbIPMK to act on IP_3 *in vivo* was tested by complementation of a *null* mutant for its ortholog *ARG82* (*arg82Δ* in *Saccharomyces cerevisiae*. Fig. 3A shows the HPLC analysis of soluble inositol phosphates isolated from yeast labeled with [^{3}H]inositol. Arg82p phosphorylates IP_3 to produce IP_4 and IP_5, and in its absence there is accumulation of IP_3, instead of the accumulation of IP_6 that occurs in wild type yeast (Fig. 3A). The metabolic pathway from IP_3 to IP_6 was restored by complementation with *TbIPMK* (Fig. 3A). These results indicate that TbIPMK function as part of the IP_6 biosynthetic pathway established in yeast (York *et al.*, 1999). We also examined the ability of TbIPMK to rescue the growth defect of *arg82Δ* yeast. Complementation of *arg82Δ* with *TbIPMK* rescued their growth defect (Fig. 3B, and 3C). Therefore, TbIPMK was able to complement yeast deficient in its ortholog Arg82p, providing molecular evidence of its function. The results also suggest that the pathway for IP_5 synthesis is similar to that present in yeast with conversion of I(1,4,5)P_3 into I(1,4,5,6)P_4 and I(1,3,4,5,6)P_5, TbIPMK acting as a 3/6-kinase. This is different from the pathway for synthesis of I(1,3,4,5,6)P_5 present in humans, where the major activity of IP_4 kinase is phosphorylation at the D-5 position (Chang *et al.*, 2002).

Characterization of the inositol pentakisphosphate kinase (TbIP5K)

Although expression of polyhistidine-tagged TbIP5K was obtained in bacteria and the recombinant protein had the expected molecular mass, we were not able to detect its activity *in vitro*, even in the presence of different isomers of IP_5 (data not shown) suggesting that additional post-translational modifications are needed. In this regard, activity of human IP5K could only be obtained when expressed in insect cells (Verbsky *et al.*, 2002). However, *TbIP5K* was able to complement *null* mutant yeast deficient in its ortholog *IPK1* (*Ipk1Δ*) (Fig. 3D). Ipk1p phosphorylates IP_5 to produce IP_6, and in its absence there is accumulation of IP_5, instead of the accumulation of IP_6 that occurs in wild type yeast. The metabolic pathway from IP_5 to IP_6 was restored by complementation with *TbIP5K* (Fig. 3D). The presence of a shoulder close to the PP-IP_4 eluting peak in the mutant yeast suggests the existence of two isomeric PP-IP_4 species. We also complemented yeast mutants for both *ipk1Δ* (*IP5K*) and *kcs1Δ* (IP6K). These mutants accumulate IP_2, IP_3, IP_4, and IP_5 but no PP-IPs. While complementation with either *TbIPMK* or *TbIP6K* (not shown) alone did not change appreciably the inositol polyphosphate profile, synthesis of IP_6 was restored by complementation with *TbIP5K* alone (Fig. 3E), demonstrating that TbIP5K is the only inositol phosphate kinase identified in *T. brucei* genome that can produce IP_6.

Characterization of the inositol hexakisphosphate kinase (TbIP6K)

TbIP6K catalyzes the formation of IP_7 from IP_6. *TbIP6K* was also tagged with an HA tag using homologous recombination with the endogenous gene loci (Oberholzer *et al.*, 2006). We detected expression of the enzyme in *T. brucei* procyclic forms (PCF) by western blot analysis (Fig. 2A). Recombinant TbIP6K was found to generate PP-IP_4 from IP_5 and IP_7 from IP_6 (Fig. 4A). Interestingly TbIP6K was not able to generate IP_8 using a 5PP-IP_7 as substrate, which suggests that, as IP6K from yeast and mammals, TbIP6K phosphorylates phosphate position D-5. Therefore, TbIP6K is able to generate two PP-IPs *in vitro*: PP-IP_4, and IP_7. The activity of TbIP6K was tested *in vivo* by complementation of a *null* mutant for its IP6K ortholog (*KCS1)* in *S. cerevisiae*. In the absence of *KCS1* there is no accumulation of IP_7, but the metabolic pathway from IP_6 to IP_7 is restored by complementation with *TbIP6K* (Fig. 4B). Complementation of *Kcs1Δ TbIP6K* also rescued the growth defect of these mutants (Fig. 4C and 4D). The TbIP6K enzymatic activity has optimum pH 6.0–7.0 (Fig. 4E).

Characterization of inositol phosphates from T. brucei cells

Previous attempts to characterize soluble inositol phosphates from *T. brucei* (Moreno *et al.*, 1992) and *T. cruzi* (Docampo *et al.*, 1991) only detected IP, IP_2 and IP_3. We used increased labeling time to 40 hours (BSF) and 75 hours (PCF) with [^{3}H]inositol and used an improved protocol for purifying and analyzing inositol phosphates (see Materials and methods). Using these conditions, we were able to detect a small peak of IP_6 in PCF but not in BSF of the parasite (Figs. 5A, and 5B). The inability to detect radiolabeled IP_6 in the BSF might simply reflect the lower number of cells that can be obtained in culture. To improve the detection of IP_6 we used a different approach that does not require metabolic labeling with [^{3}H]inositol. We extracted IPs from large amounts of cells (see Materials and methods) and assayed extracts by 35% polyacrylamide gel electrophoresis (PAGE). A band that runs like the IP_6 standard and that disappears after treatment of the extracts with phytase (Phy) was observed in both PCF and BSF (Figs. 5C, and 5D). Other highly phosphorylated inositol phosphates were not detected. These results confirm that both PCF and BSF TbIPMK and TbIP5K can sequentially synthesize IP_6 in *T. brucei.*

Biological relevance of the TbIPMK pathway

Yeast lacking Arg82p have no observable inorganic polyphosphate accumulation (Lonetti *et al.*, 2011). As polyphosphate has important roles in trypanosomes, including growth, response to osmotic stress, and maintenance of persistent infections (Lander *et al.*, 2016), we investigated whether deletion of soluble inositol polyphosphates affected the levels of polyphosphate in *T. brucei*. We used the *TbIPMK* conditional knockout BSF cell line previously described (Cestari *et al.*, 2015). Removal of tetracycline to induce the knockdown of *TbIPMK* dramatically reduced its expression more than 100-fold (Fig. 6A). Growth stalled after the first day without tetracycline (Fig. 6B). A resulting progressive reduction in polyphosphate levels was detected (Fig. 6C). Acidocalcisomes are the main cellular storage compartment for polyphosphate in trypanosomes (Lander *et al.*, 2016). However, examination of the cells by super-resolution microscopy with antibodies against the vacuolar proton pyrophosphatase (TbVP1) showed no apparent difference in labeling or distribution

of acidocalcisomes between control and *TbIPMK* mutant cells (Figure S1). In previous work we demonstrated that a knockdown of the TbVtc4, which catalyzes the synthesis and translocation of polyphosphate into acidocalcisomes, results in less electron-dense organelles, as examined by electron microscopy (Ulrich et al., 2014). We hypothesized that if the polyphosphate reduction observed (Fig. 6C) was primarily within acidocalcisomes, we should observe similar changes in the *TbIPMK* mutant cells. Indeed, electron microscopy of the *TbIPMK* mutants showed a reduction in the number (Fig. 6D), size, and electron density (compare Fig. 6E and 6F) of electron-dense organelles identifiable as acidocalcisomes. This result indicates that acidocalcisome polyphosphate synthesis is disrupted by ablation of the inositol phosphate signaling pathway.

Discussion

Our work establishes the presence of an inositol pyrophosphate (PP-IPs) synthesis pathway in *T. brucei*. We demonstrated that genes encoding proteins with homology to kinases involved in the generation of IP_5 from IP_4 and IP_3 (TbIPMK), of IP_6 from IP_5 (TbIP5K), and of IP_7 from IP_6 (TbIP6K) are present in the *T. brucei* genome (*TbIPMK, TbIP5K*, and *TbIP6K*). To demonstrate that these genes encode for functional enzymes we complemented yeast strains deficient in their corresponding orthologs and compared their products with those produced in the wild type strain providing *in vivo* genetic evidence of their function. We did not compare them with the knockout strains overexpressing the endogenous genes because the heterologous gene expression is often hampered by a diverse genetic code usage and by the lack of yeast specific post-translational processing. Thus, the heterologous genes are regularly expressed from a stronger promoter. The overexpressing of the endogenous gene from a stronger promoter might generate, to the contrary, ‘hyper’ phenotype and not a normal WT phenotype and our aim was to demonstrate their function and not to compare the activities to those of the overexpressed endogenous genes. Suppression of this pathway in *T. brucei* BSF resulted in a significant decrease in polyphosphate levels and in morphological alterations of the acidocalcisomes. The results suggest that this pathway is important for polyphosphate synthesis in acidocalcisomes.

Examination of the protein sequences of TbIPMK, TbIP5K, and TbIP6K indicated low identity with the mammalian enzymes but conservation of the putative binding site that catalyzes the transfer of phosphate from ATP to IPs, as well as of other domains required for enzymatic activity. The expression of these three kinases is very low in BSF since no clear bands were detected by western blot analyses of endogenous tagged lines, although gene expression is detectable at the mRNA level. Conversely, all three kinases can be easily identified by western blot analysis of PCF. Our results suggest, in agreement with the presence of these enzymes in other unicellular organisms such as *D. discoideum* (Europe-Finner *et al.*, 1991, Mayr GW, 1992, Stephens *et al.*, 1993), and *E. histolytica* (Martin *et al.*, 1993), an early emergence of this pathway preceding the origin of multicellularity.

The application of polyacrylamide gel electrophoresis (PAGE) and toluidine blue staining (Losito *et al.*, 2009, Pisani *et al.*, 2014) allowed the characterization of the IPs synthesizing kinases of *T. brucei* and the identification of the products of each reaction bypassing the

need for extraction under the strong acidic conditions required for HPLC analysis that has been shown to degrade some of the most highly phosphorylated species (Losito *et al.*, 2009).

Previous work has indicated that TbIPMK is essential for growth (Cestari *et al.*, 2015) and infectivity (Cestari *et al.*, 2016) of *T. brucei* BSF, and partially characterized the recombinant enzyme (Cestari *et al.*, 2016). We confirmed that TbIPMK prefers I(1,4,5)P_3 and I(1,3,4,5)P_4 as substrates (Cestari *et al.*, 2016) and found that it does not phosphorylate I(1,3,4)P_3. We also confirmed that TbIPMK cannot phosphorylate the lipid PIP_2 to PIP_3 (Cestari *et al.*, 2016), as the human enzyme does (Resnick *et al.*, 2005). In addition, we found that the enzyme can use I(1,3,4,5)P_4 and I(1,4,5,6)P_4 for the generation of I(1,3,4,5,6)P_5 indicating that TbIPMK has a dual 3-kinase/6-kinase activity. This is in contrast to the human enzyme, where the major activity of IP_4 kinase is phosphorylation at the D-5 position (Chang *et al.*, 2002). Moreover, we demonstrated that TbIPMK is able to generate PP-IP_4 *in vitro*, using either I(1,4,5)P_3, I(1,3,4,5)P_4 or I(1,3,4,5,6)P_5, as well as IP_6 from I(1,2,4,5,6)P_5, or (I(1,2,3,4,5)P_5 as substrate, again indicating a 3/6-kinase activity. TbIPMK has a neutral pH optimum for phosphorylation of both IP_3 and IP_4. Previous work (Cestari *et al.*, 2016) described inhibitors of this enzyme that inhibited *T. brucei* BSF growth. However, their IC_{50}s against the enzymes were higher (3.4–5.33 μM) than the EC_{50}s for their growth inhibition (0.51–0.83 μM), suggesting that either the drugs are accumulated or other targets might be involved in the sensitivity of *T. brucei* BSF to those inhibitors. The search for more specific inhibitors is warranted to demonstrate the relevance of this pathway to human disease and drug therapy. Interestingly, a recombinant multi-domain protein from *Plasmodium knowlesi* termed PkIPK1 was shown to have IPMK-like activity and was able to generate I(1,3,4,5)P_4 from I(1,4,5)P_3 and I(1,2,4,5,6)P_5 from either I(1,2,5,6)P_4 or I(1,3,4,6)P_4, showing 3/5-kinase activity (Stritzke *et al.*, 2012).

We were not able to detect activity of the recombinant IP5K in the presence of different isomers of IP_5 suggesting that, as proposed for the mammalian enzyme, post-translational modifications are needed for its activity (Verbsky *et al.*, 2002). However, *TbIP5K* was able to complement *null* mutant yeast deficient in its ortholog *IPK1* (*Ipk1Δ*), providing genetic evidence of its function.

Recombinant TbIP6K was able to generate PP-IP_4 from IP_5 and IP_7 from IP_6, but was not able to generate IP_8 using a 5-PP-IP_5 as substrate suggesting that, as IP6K from mammalian cells (Draskovic *et al.*, 2008), TbIP6K phosphorylates phosphate at position D-5. Therefore, TbIP6K is able to generate two PP-IPs in vitro: PP-IP_4, and IP_7. Complementation of yeast deficient in its ortholog confirmed the function of this enzyme.

T. brucei incorporates poorly the radioactive tracer [^{3}H]inositol a feature previously observed in *Dictyostelium discoideum* (Losito *et al.*, 2009). Nevertheless, improved metabolic labeling with [^{3}H]inositol resulted in detection of IP, IP_2, IP_3 and IP_6 by HPLC analysis of PCF extracts. In contrast to the results obtained using similar methods in yeasts (Azevedo *et al.*, 2006), plants (Phillippy *et al.*, 2015) or animal cells (Guse *et al.*, 1993), only very low levels of IP_6 were detected and no labeled IP_6 was detected by HPLC using BSF extracts. However, IP_6 was clearly detected by PAGE and toluidine blue staining when large numbers of parasites were used. No inositol pyrophosphates were detected since to purify

and visualize IPs we removed the abundant inorganic polyphosphate (polyP) by acidic treatment, procedure that would degrade IP_7 to IP_6. However, the absence of IP_7 could be also attributed to the high turnover of these important signaling molecules (Glennon *et al.*, 1993, Burton *et al.*, 2009). Some cells accumulate IP_6 and produce IP_7 upon signaling events. For instance, *Cryptococcus neoformans* requires synthesis of IP_7 for successful establishment of infection (Li *et al.*, 2016). A recent study demonstrated that IP_7 binds the SPX domain of proteins involved in phosphate homeostasis in plants, yeast and humans with high affinity and specificity and postulated the role of this domain as a polyphosphate sensor domain (Wild *et al.*, 2016, Azevedo *et al.*, 2017). Two proteins in *T. brucei* possess SPX domains, TbVtc4 (Lander *et al.*, 2013), which is involved in polyphosphate synthesis and translocation, and TbPho91 (Huang *et al.*, 2014), a phosphate transporter. Both proteins localize to acidocalcisomes (Huang *et al.*, 2014), the main polyphosphate storage of these cells. Our results, showing lower levels of polyphosphate and altered acidocalcisomes in *TbIPMK* BSF mutants, support the link between PP-IPs and polyphosphate metabolism.

In summary, both recombinant enzymes, TbIPMK and TbIP6K, are able to generate inositol pyrophosphates. The essentiality of the first enzyme of this pathway, TbIPMK, for growth and infectivity of *T. brucei* BSF (Cestari *et al.*, 2015, Cestari *et al.*, 2016) suggests that the study of the PP-IPs pathway in trypanosomes could lead to the elucidation of potentially multiple important roles of these compounds, possibly linked to the synthesis of polyphosphate. Differences between mammalian and trypanosome metabolism of these compounds could provide potential targets for drug development.

Experimental procedures

Chemicals and reagents

Mouse antibodies against HA were from Covance (Hollywood, FL). Inositol, myo-[1,2-^{3}H(N)] (60 Ci/mmol, ART 0261A) was from American Radiolabeled Chemicals, Inc. Goat anti-mouse antibodies were from LI-COR Biosciences (Lincoln, NE). Laemmli sample buffer was from Bio-Rad Laboratories (Hercules, CA). The bicinchoninic (BCA) protein assay kit was from Pierce (Thermo Fisher Scientific, USA). Titanium dioxide (TiO_2) beads (Titansphere ToO 5 μm) were from GL Sciences (USA). PrimeSTAR HS DNA polymerase was from Clontech Laboratories Inc. (Takara, Mountain View, CA). Vector pET32 Ek/LIC was from Novagen (Merck KGaA, Darmstadt, Germany). Acrylamide mix was from National Diagnostics (Chapel Hill, NC). CelLytic M cell lysis reagent, P8340 protease inhibitor, protease inhibitors, Benzonase Nuclease, antibody against c-Myc, inositol phosphates, and other analytical reagents were from Sigma-Aldrich (St. Louis, MO).

Cell cultures

T. brucei Lister strain 427 BSF and PCF were used. The BSF were cultivated at 37°C in HMI-9 medium (Hirumi *et al.*, 1989) supplemented with 10% heat inactivated fetal bovine serum (FBS, Sigma). The PCF were cultivated at 28°C in SDM-79 medium (Cunningham, 1977) supplemented with 10% heat-inactivated FBS and hemin (7.5 μg/ml). To determine the presence of IP_6 by PAGE analysis *T. brucei* BSF were also isolated from infected mice (Balb/c, female, 6–8 weeks old) and rats (Wistar, male retired breeders), as described

previously (Cross, 1975). *T. brucei IPMK* conditional knockout cell line was obtained and grown as described previously (Cestari *et al.*, 2015).

Yeast strains

The yeast strains used in this study are isogenic to DDY1810 (MATa leu2-3,112 trp1-Δ901 ura3-52 prb1-1122 pep4-3 prc1-407), except for the *ipk1*Δ*kcs1*Δ strain that is isogenic to BY4741 (MATa his3Δ1 leu2Δ0 met15Δ0 ura3Δ0) and was previously described (Saiardi *et al.*, 2002). The DDY1810 protease deficient strain is often used to increase the expression of exogenous proteins upon overexpression due to a deletion on the Pep4 protease. The generation of DDY1810 *kcs1*Δ strain was previously described (Onnebo *et al.*, 2009). The *arg82*Δ, *ipk1*Δ yeast strains in the DDY1810 genetic background were generated following standard homologous recombination techniques (Gueldener *et al.*, 2002) using oligonucleotides listed in Table S2. Initially diagnostic PCR was performed to confirm the correct integration of the deletion constructs. Subsequently, the soluble inositol polyphosphate profile of these new strains was used to phenotypically validate the correct homologous recombination event.

Epitope tagging, cloning expression and biochemical characterization of inositol phosphate kinases

We followed a one-step epitope-tagging method (Oberholzer *et al.*, 2006) to produce the C-terminal HA- or cMyc-tagging cassettes for transfection of *T. brucei* PCF (Table S2). Briefly, the tagging cassettes containing selection markers were generated for cell transfection by PCR using pMOTag4H and pMOTag33M as templates with the corresponding PCR primers of the genes (Table S2). Transfection was performed using 2.5 × 10^7 PCF parasites from log phase. Cells were harvested at 1,000 × *g* for 10 min, washed with 10 ml of ice-cold sterile Cytomix buffer (2 mM EGTA, 3 mM $MgCl_2$, 120 mM KCl, 0.5% glucose, 0.15 mM $CaCl_2$, 0.1 mg/ml bovine serum albumin, 10 mM K_2HPO_4/KH_2PO_4, 1 mM hypoxanthine, 25 mM Hepes, pH 7.6), centrifuged at 1,000 × *g* for 7 min, suspended in 0.5 ml Cytomix and transferred to an ice-cold 4 mm gap cuvette (Bio-Rad) containing 15 μg of PCR amplicon. Cuvettes were incubated 5 min on ice and immediately electroporated twice in Bio-Rad GenePulser Xcell™ Electroporation System at 1.5 kV, 25 μF. Cuvettes were kept on ice for one minute between electroporation pulses. Cell mixture was transferred to SDM-79 medium with 15% FBS. After 6 h appropriate antibiotics were added. The sequences of the three kinases *TbIPMK, TbIP5K* and *TbIP6K* were amplified from genomic DNA by PCR (Table S2) using PrimeSTAR HS DNA polymerase and cloned into ligation independent expression vector pET32 Ek/LIC, as recommended by the manufacturer. Constructs were cloned into *Escherichia coli* BL21-CodonPlus(DE3) and protein expression was induced with 1 mM isopropyl β-D-1-thiogalactopyranoside (IPTG) in Luria Bertani broth for 3 h. Protein purification was performed using affinity chromatography HIS-Select® Cartridge, according to the manufacturer's instructions. We tested activity of the kinases on commercially available substrates. Enzyme assays were performed at 37°C using approximately 50 ng of recombinant protein, 20 mM Hepes buffer, pH 7.0, 0.2–0.5 mM substrate, 6 mM $MgCl_2$, 100 mM NaCl, 1 mM dithiotreitol (DTT), 0.5 mM ATP, 10 mM phosphocreatine, and 40 U creatine kinase. Enzymatic reactions were stopped with 3 μl of 100 mM EDTA and kept on ice or frozen until further use. Reaction

products were resolved by PAGE using 35% acrylamide/bis-acrylamide 19:1 gels in Tris/Borate/EDTA (TBE) buffer as described by (Losito *et al.*, 2009). Gels were stained with toluidine blue (Losito *et al.*, 2009).

RNA quantification

The *TbIPMK* conditional knockout cell line was grown with or without 1 μg/ml tetracycline and harvested at room temperature. RNA was extracted with TRI reagent (Sigma) and used as template for cDNA synthesis with SuperScript III RNA Polymerase (ThermoFisher) and oligo-dT as recommended by the manufacturer. We then performed qRT-PCR analysis using specific primers (Table S2) and SYBR Green Supermix (Bio-Rad). Relative *TbIPMK* gene expression relative to actin was calculated using CFX Manager™ Software (Bio-Rad).

Western blot analyses

Cells were harvested, washed twice in PBS, and lysed with CelLytic M cell lysis reagent containing protease inhibitor cocktail (Sigma P8340) diluted 1:250, 1 mM EDTA, 1 mM phenylmethanesulfonyl fluoride (PMSF), 20 μM *trans*-epoxysuccinyl-L-leucylamido(4-guanidino)butane (E64) and 50 U/ml Benzonase Nuclease (Millipore). The protein concentration was determined by using a BCA protein assay kit. The total cell lysates were mixed with 2X Laemmli sample buffer at 1:1 ratio (vol/vol) and directly loaded in 10% SDS-PAGE. The separated proteins were transferred onto nitrocellulose membranes using a Bio-Rad transblot apparatus. The membranes were blocked with 5% (wt/vol) nonfat milk in PBS containing 0.5% Tween-20 (PBS-T) at 4°C overnight. The blots were incubated for 1 hour with mouse antibodies against HA (1:1000) or mouse antibodies against c-Myc (1:1000). After five washings with PBS-T the blots were incubated with goat anti-mouse antibodies at a dilution of 1:15000 and developed using an Odyssey CLx Infrared Imaging System (LI-COR) according to the manufacturer instructions.

Yeast complementation

S. cerevisiae strains generated from DDY1810 were used: *arg82Δ, ipk1Δ, kcs1Δ, ipk1Δkcs1Δ. TbIPMK, TbIP5K* and *TbIP6K* were amplified from *T. brucei* Lister 427, cloned into plasmid pADH:GST (pYES-ADH1-GST) (Azevedo *et al.*, 2009). Yeast cells were grown for 48 h in CSM plates. One colony was collected and suspended in 0.2 M lithium acetate with 25% polyethylene glycol solution and 0.1 M DTT. Cells were homogenized in 100 μl of solution with 100 ng of plasmid DNA and 5 μl of salmon sperm (Sigma D76560). Cells were incubated at 42°C for 30 min and immediately plated in CSM -URA plates. Colonies were used for further experiments.

Titanium dioxide bead extraction

We adapted the method of Wilson et al. (Wilson *et al.*, 2015) for cell extraction of inositol polyphosphates. Cells (5×10^9) were harvested and washed twice in washing buffer A with glucose (BAG, 116 mM NaCl, 5.4 mM KCl, 0.8 mM $MgSO_4$, 50 mM Hepes, ph 7.3, and 5.5 mM glucose). The pellet was then mixed with 1 M perchloric acid, resuspended by sonication (40% amplitude) for 10 s and kept at room temperature for 15 min. The sample was centrifuged art 18,000 × *g* for 5 min and the supernatant was transferred to a new tube

and boiled for 30 min to remove the large amount of polyphosphate present in *T. brucei*. Seven mg of TiO_2 beads were washed with water and 1 M perchloric acid, and added to the sample and left rotating for 30 min. Beads were centrifuged at 3,500 × *g* and inositol phosphates eluted with 1 M KOH, 10 mM EDTA. The sample was neutralized with perchloric acid and split into two. One half was digested with phytase (0.1 mg/ml) in the same medium at pH 5.0 and 37°C for 1 h. Extracts were resolved by 35% PAGE analysis as described above.

HPLC analysis

Inositol phosphate analysis was performed according to (Azevedo *et al.*, 2006). Briefly, yeast liquid cultures were diluted to OD_{600} 0.005 in inositol free media supplemented with 5 μCi/ml [^{3}H] inositol and grown overnight at 30°C with shaking. Cells were washed twice with water and immediately incubated with ice-cold 1 M perchloric acid and 3 mM EDTA. Glass beads were added and cells lysed by vortexing at 4°C for 2 min, 3 times. Lysates were centrifuged and supernatants neutralized with 1 M K_2CO_3 and 3 mM EDTA. Samples were analyzed by strong anion exchange HPLC using SAX 4.6125 mm column (Whatman cat. no. 4621-0505). The column was eluted with two slightly different gradients generated by mixing buffer A (1 mM Na_2EDTA) and buffer B [buffer A plus 1.3 M $(NH_4)_2HPO_4$ (pH 3.8 with H_3PO_4)] as follows: 0–5 min, 0% B; 5–10 min, 0–30% B; 10–60 min, 30–100% B; 60–80 min, 100% B; or as follow: 0–5 min, 0% B; 5–10 min, 0–10% B; 10–85 min, 20–100% B; 85–100 min 100% B. Four mL of Ultima-Flo AP liquid scintillation cocktail (Perkin-Elmer cat. no. 6013599) was added to each fraction, mixed and radioactivity quantified in a scintillation counter.

T. brucei labeling for HPLC analysis

T. brucei PCF (~3×10^6 cells) were labeled with 5 μCi/ml of 1,2-[^{3}H]-inositol in SDM-79 medium (with 10% FBS) and grown for approximately 72 h. *T. brucei* BSF (~2×10^5 cells) were labeled with 5 μCi/ml of 1,2-[^{3}H]-inositol in HMI-9 medium (with 10% FBS) and grown for approximately 40 h. Cells were washed with PBS or BAG twice and frozen immediately. Soluble inositol phosphates were extracted and analyzed as described before (Azevedo *et al.*, 2006), with minor modifications. Briefly, cells were suspended in ice-cold perchloric acid and broken by vortexing for 2 min. All steps were performed at 4°C. Lysates were centrifuged for 5 min at 18,000 × *g* and supernatants transferred to new tubes, where the pH was neutralized with 1 M K_2CO_3 and 3 mM EDTA. Samples were stored at 4°C and resolved by HPLC.

Polyphosphate extraction and measurement

Short chain polyphosphate was extracted from BSF *T. brucei* and quantified as described previously (Ulrich *et al.*, 2014).

Immunofluorescence Assay

T. brucei BSF were washed with BAG and fixed with 2% paraformaldehyde in BAG for 1 h at room temperature. Then they were adhered to poly-L-lysine coated coverslips and permeabilized with 0.1% Triton X-100 in PBS for 5 min. Blocking was performed overnight

at 4°C in PBS containing 100 mM NH_4Cl, 3% BSA, 1% fish gelatin and 5% goat serum. Cells were then incubated with anti-TbVP1 polyclonal Guinea pig antibody (1:100) for 1 h and subsequently with Alexa 488-conjugated goat anti-Guinea pig antibody (1:1000) for 1h. Microscopy images were taken with a 100X oil immersion objective, a high-power solid-state 405 nm laser and EM-CCD camera (Andor iXon) under nonsaturating conditions in a Zeiss ELYRA S1 (SR-SIM) super resolution microscope. Images were acquired and processed with ZEN 2011 software with SIM analysis module.

Electron microscopy

Imaging of whole *T. brucei* BSF and determination of morphometric parameters were done as described previously (Ulrich *et al.*, 2014).

Statistical analysis

All experiments were repeated at least three times (biological replicates) with several technical replicates as indicated in the figure legends, and where indicated results are expressed as means ± s.d. or s.e.m. of n experiments. Statistical analyses were performed using the Student's t-test. Results are considered significant when $P < 0.05$.

Supplementary Material

Refer to Web version on PubMed Central for supplementary material.

Acknowledgments

We thank Noelia Lander for help with pET32 cloning, Thomas Seebeck for the pMOTag vectors, Igor Cestari and Ken Stuart for the *TbIPMK* conditional knockout cell line, Muthugapatti Kandasamy and the Biomedical Microscopy Core of the University of Georgia for help with the super-resolution microscope, and John Shields and Mary Ard from the Georgia Electron Microscopy for help with electron microscopy. This work was funded by U.S. National Institutes of Health (grant AI077538) and supported by the Medical Research Council (MRC) core support to the MRC/UCL Laboratory for Molecular Cell Biology University Unit (MC_UU_1201814). C.C was partially supported by an European Molecular Biology Organization (EMBO) Short Term Fellowship and Center for Tropical and Emerging Global Diseases (CTEGD) travel fellowship.

References

Albert C, Safrany ST, Bembenek ME, Reddy KM, Reddy K, Falck J, et al. Biological variability in the structures of diphosphoinositol polyphosphates in *Dictyostelium discoideum* and mammalian cells. Biochem J. 1997; 327:553–560. [PubMed: 9359429]

Azevedo C, Burton A, Ruiz-Mateos E, Marsh M, Saiardi A. Inositol pyrophosphate mediated pyrophosphorylation of AP3B1 regulates HIV-1 Gag release. Proc Nat Acad Sci USA. 2009; 106:21161–21166. [PubMed: 19934039]

Azevedo C, Saiardi A. Extraction and analysis of soluble inositol polyphosphates from yeast. Nat Prot. 2006; 1:2416–2422.

Azevedo C, Saiardi A. Eukaryotic Phosphate Homeostasis: The Inositol Pyrophosphate Perspective. Trends Biochem Sci. 2017; 42:219–231. [PubMed: 27876550]

Berridge MJ. Inositol trisphosphate and calcium signalling mechanisms. Biochim Biophys Acta. 2009; 1793:933–940. [PubMed: 19010359]

Bertsch U, Deschermeier C, Fanick W, Girkontaite I, Hillemeier K, Johnen H, et al. The second messenger binding site of inositol 1,4,5-trisphosphate 3-kinase is centered in the catalytic domain and related to the inositol trisphosphate receptor site. j Biol Chem. 2000; 275:1557–1564. [PubMed: 10636844]

Burton A, Azevedo C, Andreassi C, Riccio A, Saiardi A. Inositol pyrophosphates regulate JMJD2C-dependent histone demethylation. Proc Nat Acad Sci USA. 2013; 110:18970–18975. [PubMed: 24191012]

Burton A, Hu X, Saiardi A. Are inositol pyrophosphates signalling molecules? J Cell Physiol. 2009; 220:8–15. [PubMed: 19326391]

Cestari I, Haas P, Moretti NS, Schenkman S, Stuart K. Chemogenetic characterization of inositol ophosphate metabolic pathway reveals druggable enzymes for targeting kinetoplastid parasites. Cell Chem Biol. 2016; 23:608–617. [PubMed: 27133314]

Cestari I, Stuart K. Inositol phosphate pathway controls transcription of telomeric expression sites in trypanosomes. Proc Nat Acad Sci USA. 2015; 112:E2803–2812. [PubMed: 25964327]

Chang SC, Miller AL, Feng Y, Wente SR, Majerus PW. The human homolog of the rat inositol phosphate multikinase is an inositol 1,3,4,6-tetrakisphosphate 5-kinase. J Biol Chem. 2002; 277:43836–43843. [PubMed: 12223481]

Choi JH, Williams J, Cho J, Falck JR, Shears SB. Purification, sequencing, and molecular identification of a mammalian PP-InsP5 kinase that is activated when cells are exposed to hyperosmotic stress. J Biol Chem. 2007; 282:30763–30775. [PubMed: 17702752]

Cocco L, Follo MY, Manzoli L, Suh PG. Phosphoinositide-specific phospholipase C in health and disease. J Lipid Res. 2015; 56:1853–1860. [PubMed: 25821234]

Cross GA. Identification, purification and properties of clone-specific glycoprotein antigens constituting the surface coat of *Trypanosoma brucei*. Parasitology. 1975; 71:393–417. [PubMed: 645]

Cunningham I. New culture medium for maintenance of tsetse tissues and growth of trypanosomatids. J Protozool. 1977; 24:325–329. [PubMed: 881656]

Docampo R, Pignataro OP. The inositol phosphate/diacylglycerol signalling pathway in *Trypanosoma cruzi*. Biochem J. 1991; 275:407–411. [PubMed: 2025225]

Draskovic P, Saiardi A, Bhandari R, Burton A, Ilc G, Kovacevic M, et al. Inositol hexakisphosphate kinase products contain diphosphate and triphosphate groups. Chem Biol. 2008; 15:274–286. [PubMed: 18355727]

Europe-Finner GN, Gammon B, Newell PC. Accumulation of [^{3}H]-inositol into inositol polyphosphates during development of *Dictyostelium*. Biochem Biophys Res Commun. 1991; 181:191–196. [PubMed: 1958187]

Ghosh S, Shukla D, Suman K, Lakshmi BJ, Manorama R, Kumar S, Bhandari R. Inositol hexakisphosphate kinase 1 maintains hemostasis in mice by regulating platelet polyphosphate levels. Blood. 2013; 122:1478–1486. [PubMed: 23782934]

Glennon MC, Shears SB. Turnover of inositol pentakisphosphates, inositol hexakisphosphate and diphosphoinositol polyphosphates in primary cultured hepatocytes. Biochem J. 1993; 293:583–590. [PubMed: 8343137]

Gokhale NA, Zaremba A, Janoshazi AK, Weaver JD, Shears SB. PPIP5K1 modulates ligand competition between diphosphoinositol polyphosphates and PtdIns(3,4,5)P_3 for polyphosphoinositide-binding domains. Biochem J. 2013; 453:413–426. [PubMed: 23682967]

Gueldener U, Heinisch J, Koehler GJ, Voss D, Hegemann JH. A second set of loxP marker cassettes for Cre-mediated multiple gene knockouts in budding yeast. Nucleic Acids Res. 2002; 30:e23. [PubMed: 11884642]

Guse AH, Greiner E, Emmrich F, Brand K. Mass changes of inositol 1,3,4,5,6-pentakisphosphate and inositol hexakisphosphate during cell cycle progression in rat thymocytes. J Biol Chem. 1993; 268:7129–7133. [PubMed: 8463248]

Hirumi H, Hirumi K. Continuous cultivation of *Trypanosoma brucei* blood stream forms in a medium containing a low concentration of serum protein without feeder cell layers. J Parasitol. 1989; 75:985–989. [PubMed: 2614608]

Huang G, Bartlett PJ, Thomas AP, Moreno SN, Docampo R. Acidocalcisomes of *Trypanosoma brucei* have an inositol 1,4,5-trisphosphate receptor that is required for growth and infectivity. Proc Nat Acad Sci USA. 2013; 110:1887–1892. [PubMed: 23319604]

Huang G, Ulrich PN, Storey M, Johnson D, Tischer J, Tovar JA, et al. Proteomic analysis of the acidocalcisome, an organelle conserved from bacteria to human cells. PLoS Pathog. 2014; 10:e1004555. [PubMed: 25503798]

Illies C, Gromada J, Fiume R, Leibiger B, Yu J, Juhl K, et al. Requirement of inositol pyrophosphates for full exocytotic capacity in pancreatic beta cells. Science. 2007; 318:1299–1302. [PubMed: 18033884]

Irvine RF, Schell MJ. Back in the water: the return of the inositol phosphates. Nature reviews Mol Cell Biol. 2001; 2:327–338.

Jadav RS, Chanduri MV, Sengupta S, Bhandari R. Inositol pyrophosphate synthesis by inositol hexakisphosphate kinase 1 is required for homologous recombination repair. J Biol Chem. 2013; 288:3312–3321. [PubMed: 23255604]

King-Keller S, Moore CA, Docampo R, Moreno SN. Ca^{2+} regulation of *Trypanosoma brucei* phosphoinositide phospholipase C. Eukaryot Cell. 2015; 14:486–494. [PubMed: 25769297]

Laha D, Johnen P, Azevedo C, Dynowski M, Weiss M, Capolicchio S, et al. VIH2 regulates the synthesis of inositol pyrophosphate $InsP_8$ and jasmonate-dependent defenses in *Arabidopsis*. Plant Cell. 2015; 27:1082–1097. [PubMed: 25901085]

Lander N, Cordeiro C, Huang G, Docampo R. Polyphosphate and acidocalcisomes. Biochem Soc Trans. 2016; 44:1–6. [PubMed: 26862180]

Lander N, Ulrich PN, Docampo R. *Trypanosoma brucei* vacuolar transporter chaperone 4 (TbVtc4) is an acidocalcisome polyphosphate kinase required for in vivo infection. J Biol Chem. 2013; 288:34205–34216. [PubMed: 24114837]

Li C, Lev S, Saiardi A, Desmarini D, Sorrell TC, Djordjevic JT. Identification of a major IP_5 kinase in *Cryptococcus neoformans* confirms that PP-IP_5/IP_7, not IP_6, is essential for virulence. Sci Rep. 2016; 6:23927. [PubMed: 27033523]

Lonetti A, Szijgyarto Z, Bosch D, Loss O, Azevedo C, Saiardi A. Identification of an evolutionarily conserved family of inorganic polyphosphate endopolyphosphatases. J Biol Chem. 2011; 286:31966–31974. [PubMed: 21775424]

Losito O, Szijgyarto Z, Resnick AC, Saiardi A. Inositol pyrophosphates and their unique metabolic complexity: analysis by gel electrophoresis. PLoS One. 2009; 4:e5580. [PubMed: 19440344]

Luo HR, Huang YE, Chen JC, Saiardi A, Iijima M, Ye K, et al. Inositol pyrophosphates mediate chemotaxis in *Dictyostelium* via pleckstrin homology domain-PtdIns(3,4,5)P_3 interactions. Cell. 2003; 114:559–572. [PubMed: 13678580]

Luo HR, Saiardi A, Yu H, Nagata E, Ye K, Snyder SH. Inositol pyrophosphates are required for DNA hyperrecombination in protein kinase c1 mutant yeast. Biochemistry. 2002; 41:2509–2515. [PubMed: 11851397]

Martin JB, Bakker-Grunwald T, Klein G. ^{31}P-NMR analysis of *Entamoeba histolytica*. Occurrence of high amounts of two inositol phosphates. Eur J Biochem. 1993; 214:711–718. [PubMed: 8319681]

Mayr GWRT, THiel U, Vogel G, Stephens LR. Phosphoinositol diphosphates: non-enzymic formation in vitro and occurrence in vivo in the cellular slime mold *Dictysotelium*. Carbohyd Res. 1992; 234:247–262.

Menniti FS, Miller RN, Putney JW Jr, Shears SB. Turnover of inositol polyphosphate pyrophosphates in pancreatoma cells. J Biol Chem. 1993; 268:3850–3856. [PubMed: 8382679]

Moreno SN, Docampo R, Vercesi AE. Calcium homeostasis in procyclic and bloodstream forms of *Trypanosoma brucei*. Lack of inositol 1,4,5-trisphosphate-sensitive Ca^{2+} release. J Biol Chem. 1992; 267:6020–6026. [PubMed: 1556113]

Morrison BH, Bauer JA, Kalvakolanu DV, Lindner DJ. Inositol hexakisphosphate kinase 2 mediates growth suppressive and apoptotic effects of interferon-beta in ovarian carcinoma cells. J Biol Chem. 2001; 276:24965–24970. [PubMed: 11337497]

Nagata E, Luo HR, Saiardi A, Bae BI, Suzuki N, Snyder SH. Inositol hexakisphosphate kinase-2, a physiologic mediator of cell death. J Biol Chem. 2005; 280:1634–1640. [PubMed: 15533939]

Nagata E, Saiardi A, Tsukamoto H, Satoh T, Itoh Y, Itoh J, et al. Inositol hexakisphosphate kinases promote autophagy. Int J Biochem & Cell Biol. 2010; 42:2065–2071. [PubMed: 20883817]

Nalaskowski MM, Deschermeier C, Fanick W, Mayr GW. The human homologue of yeast ArgRIII protein is an inositol phosphate multikinase with predominantly nuclear localization. Biochem J. 2002; 366:549–556. [PubMed: 12027805]

Nishizuka Y. Studies and perspectives of protein kinase C. Science. 1986; 233:305–312. [PubMed: 3014651]

Oberholzer M, Morand S, Kunz S, Seebeck T. A vector series for rapid PCR-mediated C-terminal in situ tagging of *Trypanosoma brucei* genes. Mol biochem Parasitol. 2006; 145:117–120. [PubMed: 16269191]

Onnebo SM, Saiardi A. Inositol pyrophosphates modulate hydrogen peroxide signalling. Biochem J. 2009; 423:109–118. [PubMed: 19614566]

Pesesse X, Choi K, Zhang T, Shears SB. Signaling by higher inositol polyphosphates. Synthesis of bisdiphosphoinositol tetrakisphosphate ("$InsP_8$") is selectively activated by hyperosmotic stress. J Biol Chem. 2004; 279:43378–43381. [PubMed: 15316027]

Phillippy BQ, Perera IY, Donahue JL, Gillaspy GE. Certain malvaceae plants have a unique accumulation of myo-Inositol 1,2,4,5,6-pentakisphosphate. Plants (Basel). 2015; 4:267–283. [PubMed: 27135328]

Pisani F, Livermore T, Rose G, Chubb JR, Gaspari M, Saiardi A. Analysis of *Dictyostelium discoideum* inositol pyrophosphate metabolism by gel electrophoresis. PLoS One. 2014; 9:e85533. [PubMed: 24416420]

Prasad A, Jia Y, Chakraborty A, Li Y, Jain SK, Zhong J, et al. Inositol hexakisphosphate kinase 1 regulates neutrophil function in innate immunity by inhibiting phosphatidylinositol-(3,4,5)-trisphosphate signaling. Nat Immunol. 2011; 12:752–760. [PubMed: 21685907]

Resnick AC, Snowman AM, Kang BN, Hurt KJ, Snyder SH, Saiardi A. Inositol polyphosphate multikinase is a nuclear PI_3-kinase with transcriptional regulatory activity. Proc Nat Acad Sci USA. 2005; 102:12783–12788. [PubMed: 16123124]

Saiardi A. Cell signalling by inositol pyrophosphates. Subcell Biochem. 2012; 59:413–443. [PubMed: 22374099]

Saiardi A, Caffrey JJ, Snyder SH, Shears SB. The inositol hexakisphosphate kinase family. Catalytic flexibility and function in yeast vacuole biogenesis. J Biol Chem. 2000; 275:24686–24692. [PubMed: 10827188]

Saiardi A, Nagata E, Luo HR, Sawa A, Luo X, Snowman AM, Snyder SH. Mammalian inositol polyphosphate multikinase synthesizes inositol 1,4,5-trisphosphate and an inositol pyrophosphate. Proc Nat Acad Sci USA. 2001a; 98:2306–2311. [PubMed: 11226235]

Saiardi A, Resnick AC, Snowman AM, Wendland B, Snyder SH. Inositol pyrophosphates regulate cell death and telomere length through phosphoinositide 3-kinase-related protein kinases. Proc Nat Acad Sci USA. 2005; 102:1911–1914. [PubMed: 15665079]

Saiardi A, Sciambi C, McCaffery JM, Wendland B, Snyder SH. Inositol pyrophosphates regulate endocytic trafficking. Proc Nat Acad Sci USA. 2002; 99:14206–14211. [PubMed: 12391334]

Shears SB. Inositol pyrophosphates: why so many phosphates? Adv Biol Reg. 2015; 57:203–216.

Stephens L, Radenberg T, Thiel U, Vogel G, Khoo KH, Dell A, et al. The detection, purification, structural characterization, and metabolism of diphosphoinositol pentakisphosphate(s) and bisdiphosphoinositol tetrakisphosphate(s). J Biol Chem. 1993; 268:4009–4015. [PubMed: 8440693]

Stritzke C, Nalaskowski MM, Fanick W, Lin H, Mayr GW. A *Plasmodium* multi-domain protein possesses multiple inositol phosphate kinase activities. Mol Biochem Parasitol. 2012; 186:134–138. [PubMed: 23123170]

Szijgyarto Z, Garedew A, Azevedo C, Saiardi A. Influence of inositol pyrophosphates on cellular energy dynamics. Science. 2011; 334:802–805. [PubMed: 22076377]

Ulrich PN, Lander N, Kurup SP, Reiss L, Brewer J, Soares Medeiros LC, et al. The acidocalcisome vacuolar transporter chaperone 4 catalyzes the synthesis of polyphosphate in insect-stages of *Trypanosoma brucei* and *T. cruzi*. J Eukaryot Microbiol. 2014; 61:155–165. [PubMed: 24386955]

Urbaniak MD, Martin DM, Ferguson MA. Global quantitative SILAC phosphoproteomics reveals differential phosphorylation is widespread between the procyclic and bloodstream form lifecycle stages of *Trypanosoma brucei*. J Proteome Res. 2013; 12:2233–2244. [PubMed: 23485197]

Verbsky JW, Wilson MP, Kisseleva MV, Majerus PW, Wente SR. The synthesis of inositol hexakisphosphate. Characterization of human inositol 1,3,4,5,6-pentakisphosphate 2-kinase. J Biol Chem. 2002; 277:31857–31862. [PubMed: 12084730]

Wild R, Gerasimaite R, Jung JY, Truffault V, Pavlovic I, Schmidt A, et al. Control of eukaryotic phosphate homeostasis by inositol polyphosphate sensor domains. Science. 2016; 352:986–990. [PubMed: 27080106]

Wilson MS, Bulley SJ, Pisani F, Irvine RF, Saiardi A. A novel method for the purification of inositol phosphates from biological samples reveals that no phytate is present in human plasma or urine. Open Biol. 2015; 5:150014. [PubMed: 25808508]

York JD, Odom AR, Murphy R, Ives EB, Wente SR. A phospholipase C-dependent inositol polyphosphate kinase pathway required for efficient messenger RNA export. Science. 1999; 285:96–100. [PubMed: 10390371]

York SJ, Armbruster BN, Greenwell P, Petes TD, York JD. Inositol diphosphate signaling regulates telomere length. J Biol Chem. 2005; 280:4264–4269. [PubMed: 15561716]

Zhang T, Caffrey JJ, Shears SB. The transcriptional regulator, Arg82, is a hybrid kinase with both monophosphoinositol and diphosphoinositol polyphosphate synthase activity. FEBS Lett. 2001; 494:208–212. [PubMed: 11311242]

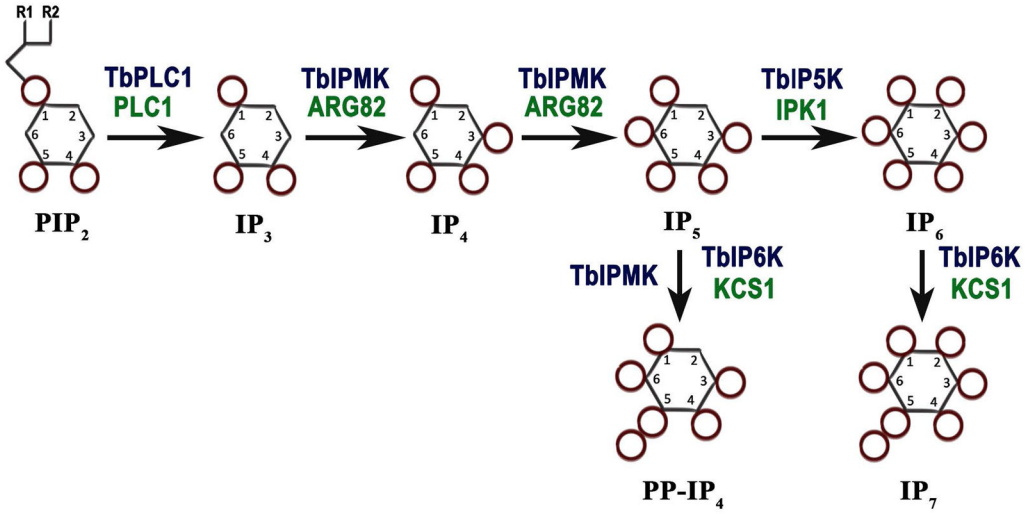

Fig. 1.

Inositol phosphate pathway in *Trypanosoma brucei*. The soluble IP pathway starts with hydrolysis of PIP_2 by TbPI-PLC1, releasing IP_3 that is phosphorylated by TbIPMK to generate IP_4 and IP_5. IP_5 is phosphorylated by TbIP5K to generate IP_6. IP_5 and IP_6 can be further phosphorylated by TbIPMK or TbIP6K to generate inositol pyrophosphates PP-IP_4 and IP_7. Names of the equivalent yeast enzymes are in green.

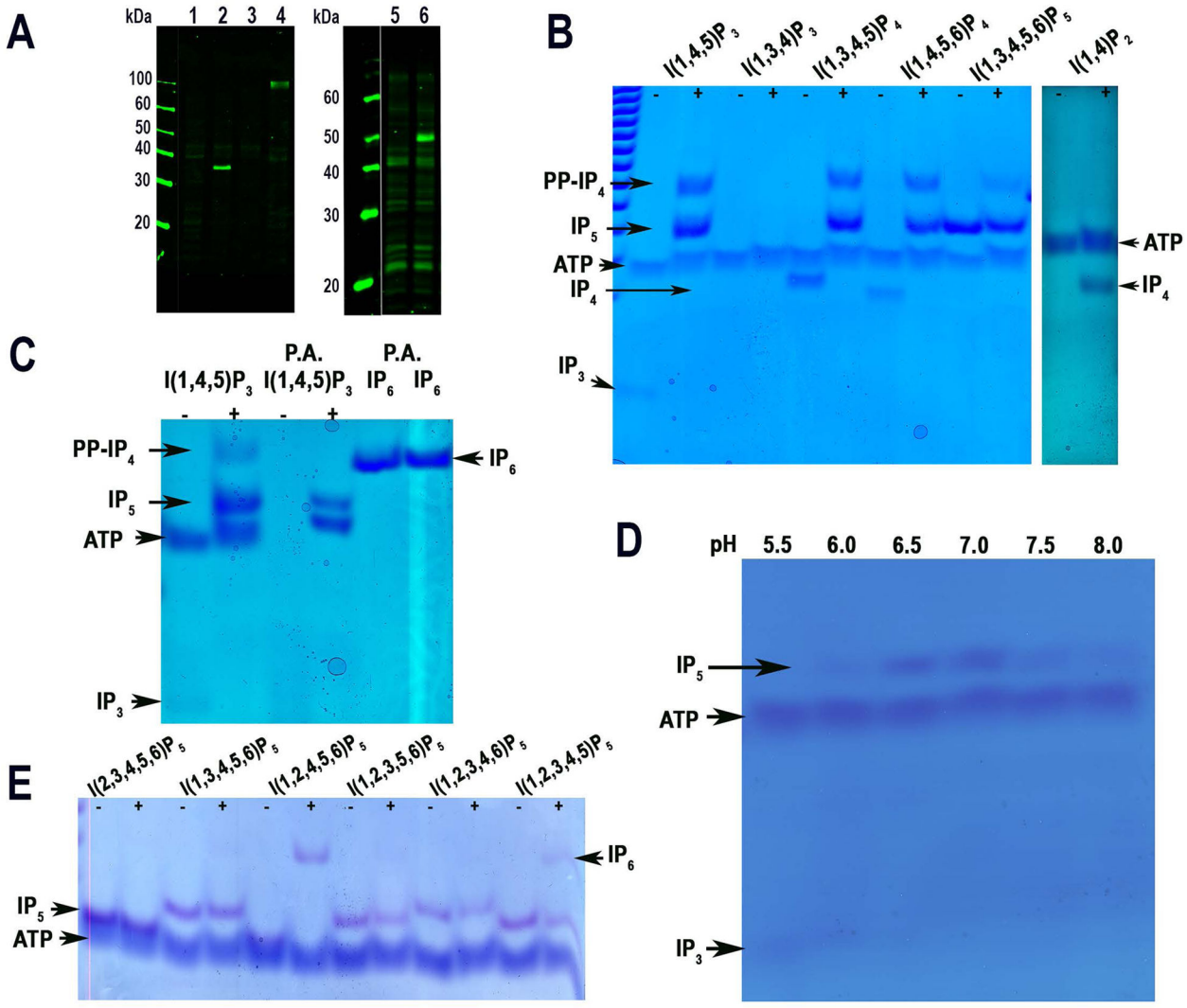

Fig. 2. Western blot analyses and enzymatic activity of TbIPMK

A. Western blot analyses of *T. brucei* PCF expressing epitope-tagged TbIPMK, TbIP5K and TbIP6K. *Left panel* are HA tagged cell lines: 1, wild-type; 2, TbIPMK-HA; 3, wild-type; 4, TbIP6K-HA. *Right panel* is a c-Myc tagged line: 5, wild-type; 6, TbIP5K-cMyc.

B. Kinase reactions performed with recombinant TbIPMK (2 μg) using the indicated substrates at 250 μM for 1 hour at 37°C. TbIPMK can phosphorylate $I(1,4,5)P_3$ but not $I(1,3,4)P_3$ to produce $I(1,3,4)P_5$ and PP-IP_4, and can phosphorylate $I(1,3,4,5)P_4$, and $I(1,4,5,6)P_4$ to produce IP_5 and PP-IP_4. It can also phosphorylate $I(1,3,4,5,6)P_5$ to PP-IP_4. Other *arrows* show bands corresponding to ATP, IP_4, and IP_3. TbIPMK can phosphorylate $I(1,4)P_2$ to produce IP_4, and $I(1,4,5)P_3$ to produce IP_5 and PP-IP_4.

C. Treatment of the sample with perchloric acid (PA) eliminates the band corresponding to PP-IP_4 but has no effect on IP_6. Other *arrows* indicate bands corresponding to ATP and IP_3.

D. Optimum pH for TbIPMK activity is within the physiological range.

E. TbIPMK can only phosphorylate positions 3 and 6 of different IP_5 derivatives to generate IP_6. Note the lower synthesis of PP-IP_4 using $I(1,3,4,5,6)P_5$ as substrate compared to results

obtained in (B) and (C). We observed that shorter enzymatic reaction time resulted in less PP-IP_4 synthesis.

All results are representative of three or more independent experiments.

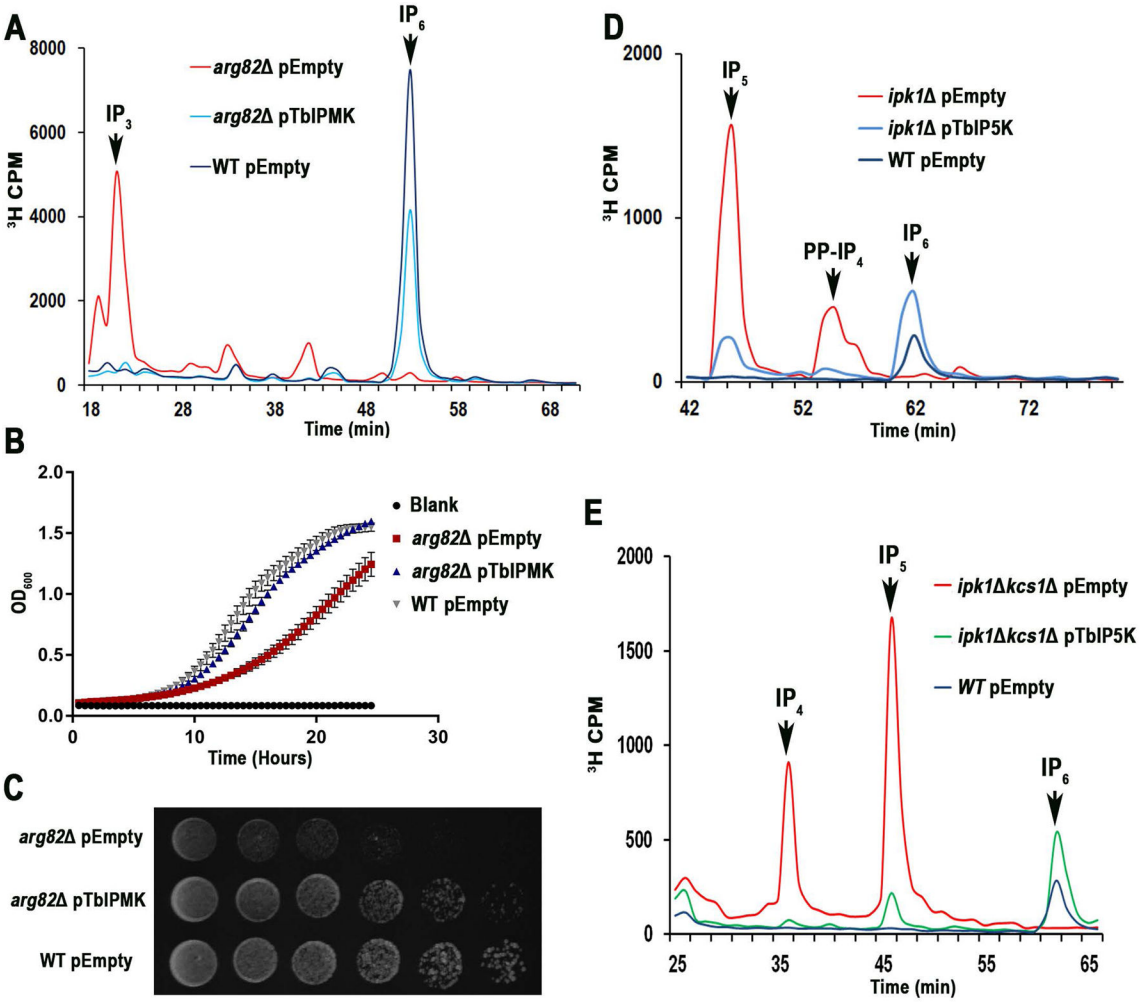

Fig. 3. *TbIPMK*, and *TbIP5K* complementation of yeast mutants

A. HPLC analysis of soluble inositol phosphates of *S. cerevisiae arg82Δ* mutants transformed with an empty vector (*red*) or a vector containing the entire open reading frame of *TbIPMK* (*blue*), and compared to those of wild-type (WT) yeast transformed with empty vector (*black*).

B. Growth of the same cells in liquid medium as estimated by measuring optical density at 660 nm. *arg82*Δ mutants had reduced growth, which was restored by expression of *TbIPMK*. Mean ± s.d. for three independent experiments, each one with 6 duplicates.

C. WT, and *arg82*Δ transformed with empty vector or *arg82*Δ transformed with *TbIPMK* (serially diluted 10-fold, 10^6–10 cells/spot from left to right) were spotted on YPD plates and incubated at 30°C for 2 days.

D. HPLC analysis of soluble inositol phosphates of *Scipk1Δ* mutants transformed with an empty vector (*red*) or a vector containing the entire open reading frame of *TbIPMK* (*blue*) and compared with wild type transformed with an empty vector (*black*).

E. HPLC analysis of *Scipk1ΔKcs1Δ* complemented with empty vector (*red*) or *TbIP5K* (*green*) shows reconstitution of IP_6 synthesis. In *black*, wild type transformed with empty vector.

All results are representative of three or more independent experiments.

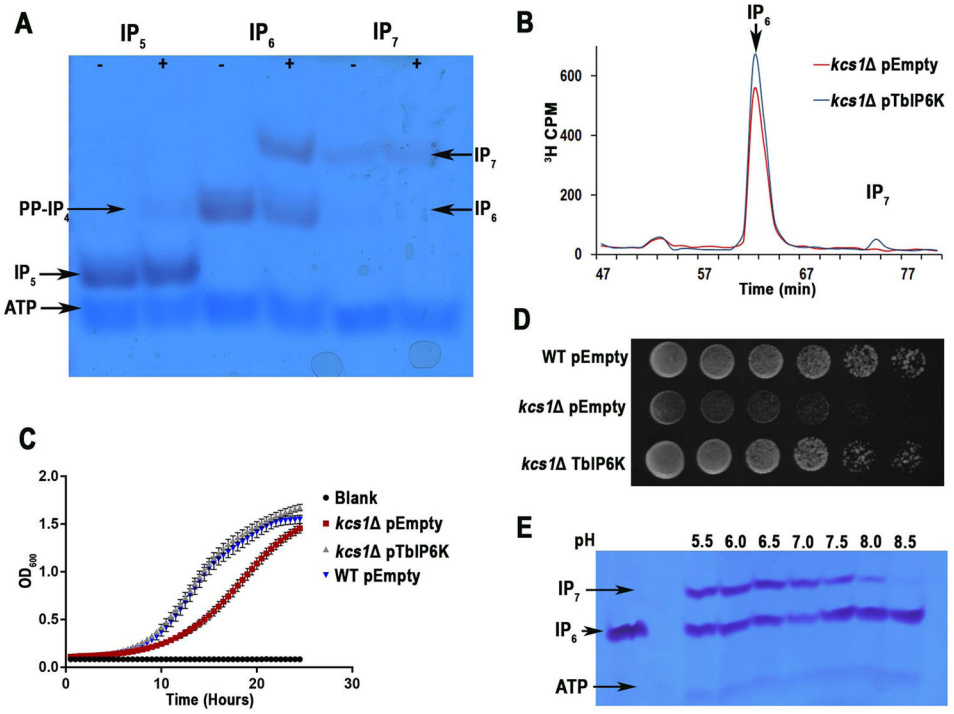

Fig. 4. TbIP6K activity and complementation of yeast mutants

A. Kinase reactions performed with recombinant TbIP6K (2 μg) using the indicated substrates at 150 μM for 1 hour at 37°C. TbIP6K can phosphorylate I(1,3,4,5,6)P_5 to PP-IP_4 and IP_6 to produce IP_7 (5PP-IP_5) but cannot phosphorylate IP_7 to produce IP_8. Other *arrows* show bands corresponding to ATP, and IP_5.

B. HPLC analysis of soluble inositol phosphates of *S. cerevisiae kcs1Δ* mutants transformed with an empty vector (*red*) or a vector containing the entire open reading frame of *TbIP6K* (*blue*).

C. Growth of the same cells in liquid medium as estimated by measuring optical density at 660 nm. *kcs1Δ* mutants had reduced growth, which was restored by expression of *TbIP6K*. Mean ± s.d. for three independent experiments, each one with 6 duplicates.

D. WT, and *kcs1Δ* transformed with empty vector or *kcs1*Δ transformed with *TbIP6K* (serially diluted 10-fold, 10^6–10 cells/spot from left to right) were spotted on YPD plates and incubated at 30°C for 2 days.

E. Optimum pH for TbIP6K activity is under acidic conditions. We detected a higher activity at pH 6.0 and 6.5.

All results are representative of three or more independent experiments.

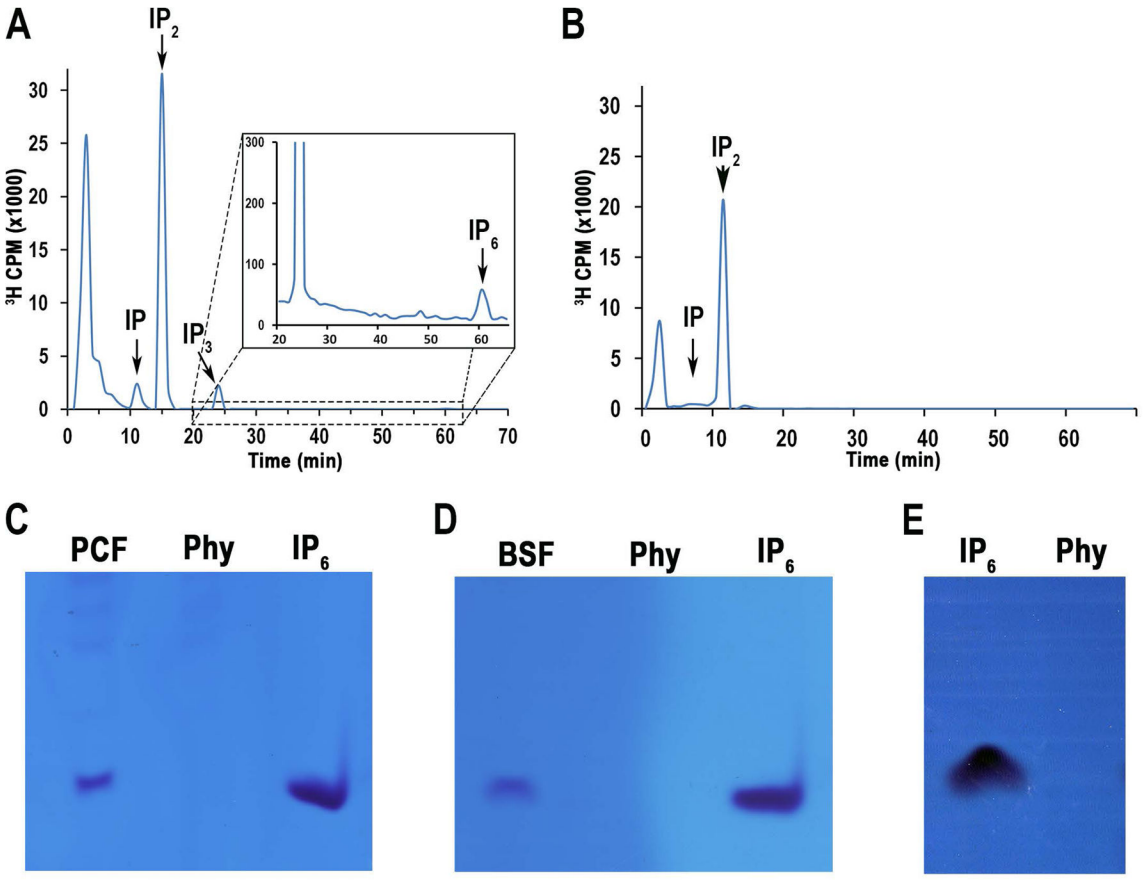

Fig. 5. HPLC and PAGE analyses of soluble inositol phosphates from *T. brucei* PCF and BSF

A. PCF showed the presence of IP, IP_2, IP_3 and IP_6.

B. BSF showed the presence of IP, and IP_2. Cells were labeled with [^{3}H]inositol as described under *Experimental Procedures*.

C–E. PAGE analyses of extracts from PCF (C) or BSF (D) or standard IP_6 (E). Samples in (C) and (D) (5×10^9 cells) were treated with phytase (Phy) (0.1 mg/ml, pH 5.0, at 37°C for 1 hour) to confirm that the bands correspond to IP_6.

E. Phytase control activity with IP_6 standard.

All results are representative of three or more independent experiments.

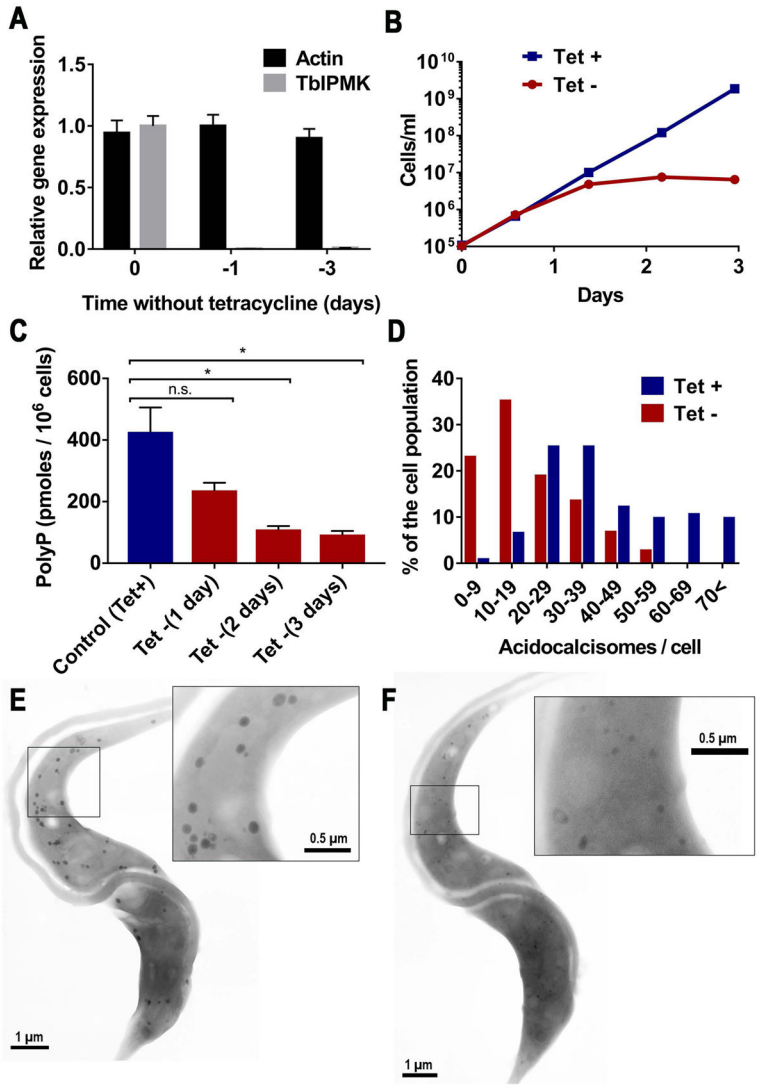

Fig. 6. Phenotypic changes of mutant BSF deficient in TbIPMK

A. qRT-PCR analysis of gene expression of *TbIPMK* at time 0 and after 1 and 3 days in the absence of tetracycline as compared to expression of control actin. Values are means ± s.e.m., $n = 3$. $P < 0.001$ at days 1 and 3 without tetracycline. Student's *t* test.

B. In vitro growth of BSF in the presence (*+Tet*) or absence (*-Tet*) of 1 μM tetracycline. Values are means ± s.e.m., $n = 3$ (bars are smaller than symbols).

C. Quantification of short-chain polyphosphate in control (*+Tet*) and induced (*-Tet*) *TbIPMK* conditional knockout BSF. Values are means ± s.e.m, $n = 3$, $^*P < 0.05$. Student's *t* test.

D. Numeric distribution of acidocalcisomes in BSF. Whole unfixed parasites were observed by transmission electron microscopy and the number of acidocalcisomes per cell in ~100 cells of control *(+Tet)* and conditional *TbIPMK* mutants (*-Tet*) were counted (the results from 3 independent experiments were combined).

E, F. Scanning transmission electron microscopy (STEM) images from control (E) or *TbIPMK* conditional mutant BSF showing acidocalcisomes. Bar = 1 μm. *Insets* show acidocalcisomes highlighted in (E) and (F) at higher magnification. Bars = 0.5 μm.